JMEPEG (2009) 18:333–338
DOI: 10.1007/s11665-008-9202-z

Investigations of Solidification Structures of High Carbon Alloy Cast Steel Containing RE-V-Ti

Hanguang Fu, Yinhu Qu, and Jiandong Xing

(Submitted May 3, 2007; in revised form November 14, 2007)

The solidification microstructural characteristics of rare earth (RE) and vanadium and titanium-treated high carbon alloy cast steel, whose chemical compositions are 0.90 wt.% C, 3.0 wt.% Si, and 1.0 wt.% Mn, were investigated by means of optical microscopy (OM), scanning electron microscopy (SEM), electron probe microanalyzer (EPMA), and energy dispersive X-ray spectrometry (EDS). The alloys were prepared in an induction furnace. The results showed that compound additions of RE-V-Ti could obviously refine the solidification structures and decrease the diameter of grains. The average grain diameter of untreated high carbon alloy cast steel was 80 μm. The average grain diameter of high carbon alloy cast steel containing RE-V-Ti decreased to 40 μm. Finally, the reasons that RE-V-Ti refined the solidification structure were analyzed in detail.

Keywords cast steel, rare earth, refinement, solidification structure, titanium

1. Introduction

Bainitic steel usually exhibits better strength, toughness, and ductility than the martensitic and pearlitic steel and was widely used in the industrial production (Ref 1-3). But, the presence of coarse carbide precipitating in the bainite gives the microstructure poor ductility and less resistance to the cleavage fracture (Ref 4). Recent studies have discovered that the precipitation of carbides from austenite can be suppressed completely by adding an appropriate concentration of silicon (Ref 5, 6). The resulting carbide-free microstructure consists of the bainitic ferrite, the retained austenite, and possibly, the martensite. The stability of the residual austenite is greatly improved by the absence of carbide, since the austenite can act as a sink of carbon, a strong austenite stabilizer. Such bainitic microstructures have higher ductility and toughness than comparable coarse carbide-containing microstructures (Ref 7-9). Furthermore, carbide-free bainitic microstructures are shown to exhibit better tensile strength, impact toughness, and comparable wear resistance (Ref 6, 10).

However, the solidification structure of high carbon alloy cast steel containing many silicon elements is coarse. High carbon alloy cast steel is easy to crack in the casting also. So far, rare earth (RE), vanadium and titanium have been widely used for the modification of microalloyed steels. By adding an appropriate concentration of RE, vanadium, and titanium, the toughness, plasticity, wear, and corrosion-resistant properties could be remarkably improved for the microalloyed steels (Ref 11-13).

Until now, few studies have focused on the combined effects of RE-V-Ti and on the refining mechanism of solidification microstructures. The interaction among RE-V-Ti influences the microstructures of high carbon alloy steel. Therefore, it is very important to investigate the influence of RE-V-Ti on the solidification microstructures of high carbon alloy steel and the segregation of alloy elements. Work on the heat treatment microstructures and mechanical properties of these materials will be the subject of future papers.

2. Experimental

A master alloy of 0.90 wt.% C alloy steel was made in a 300 kg capacity induction furnace. The melt was poured into a metallic mold and let to cool. The chemical composition of this alloy is shown in Table 1. From this master alloy, 20 kg samples of material were remelted in a 20 kg capacity furnace. The additions of modifiers were as follows: (a) No RE-V-Ti; (b) 0.25 wt.% RE only; (c) 0.15 wt.% V and 0.15 wt.% Ti; (d) 0.25 wt.% RE and 0.15 wt.% V and 0.15 wt.% Ti. The corresponding sample numbers were A_0, A_1, A_2, and A_3, respectively. These alloys were then cast at 1450 °C into sand molds to produce ingots of dimensions of $30 \times 40 \times 120$ mm. A thermocouple (Pt-Pt/Rh) was introduced through the side of the mold and was placed centrally at half the height of the mold cavity. Thermocouple output was logged and indicated a cooling rate of 2.3 °C/s. Materials were investigated in the as-cast.

The investigation techniques used for structure characterization included optical microscopy (OM), scanning electron microscopy (SEM), energy dispersive X-ray spectrometry (EDS), and electron probe microanalyzer (EPMA). Metallographic analysis were made on the samples etched in 4% natal. The optical microscope used was a Neophot 32. The SEM

Hanguang Fu and **Jiandong Xing**, State Key Laboratory for Mechanical Behavior of Materials, School of Materials Science and Engineering, Xi'an Jiaotong University, 28 Xianning West Road, Xi'an 710049, Shaanxi Province, P.R. China; and **Yinhu Qu** School of Electromechanical Engineering, Xi'an Polytechnic University, Xi'an 710048, Shaanxi Province, P.R. China. Contact e-mail: fhg64@263.net.

used was a CSM 950. Energy dispersive X-ray spectrometry (EDS) was carried on an accessory of a scanning microscope. EPMA was carried on a JXA-8800R electron probe microanalyzer. The average size of grain is obtained by image analysis using a Leica digital image analyzer.

3. Results

3.1 Effect of RE-V-Ti on the Grain Size of High Carbon Alloy Cast Steel

The grain size of high carbon alloy cast steel under different treating conditions is shown in Fig. 1. The grain of unmodified cast steel is coarse and its average size is 80 μm, as shown in Fig. 1a. Adding 0.25 wt.% RE, the grain size of the cast steel decreases obviously and reaches 65 μm, as shown in Fig. 1b. When 0.15 wt.% V and 0.15 wt.% Ti are added to the cast steel, the grain size of the cast steel decreases further and reaches 50 μm, as shown in Fig. 1c. Adding 0.25 wt.% RE and 0.15 wt.% V and 0.15 wt.% Ti, the refinement of cast steel grain is the best. The average grain size of high carbon alloy cast steel is only 40 μm, as shown in Fig. 1d.

Table 1 Chemical composition of the master alloy

Element	wt.%
Carbon	0.90
Silicon	3.07
Manganese	0.98
Molybdenum	0.29
Phosphorus	0.038
Sulfur	0.036

3.2 EPMA Analysis of High Carbon Alloy Cast Steel Sample

Figure 2 shows the EPMA analysis of unmodified high carbon alloy cast steel sample. The segregation of elements is obvious. Especially, the segregation of carbon element is very obvious, as shown in Fig. 2b. After modification with RE-V-Ti, the segregation of elements shows a lightening tendency, as shown in Fig. 3. The lightening of elements' segregation gains from the refinement of solidification structure and the increase of solidification rate. It is beneficial to the homogenization of as-cast and heat treatment structures of alloy cast steel and the improvement of mechanical properties of high carbon alloy cast steel.

4. Discussion

The main reasons that RE-V-Ti refines the solidification structure of high carbon alloy cast steel are as follows.

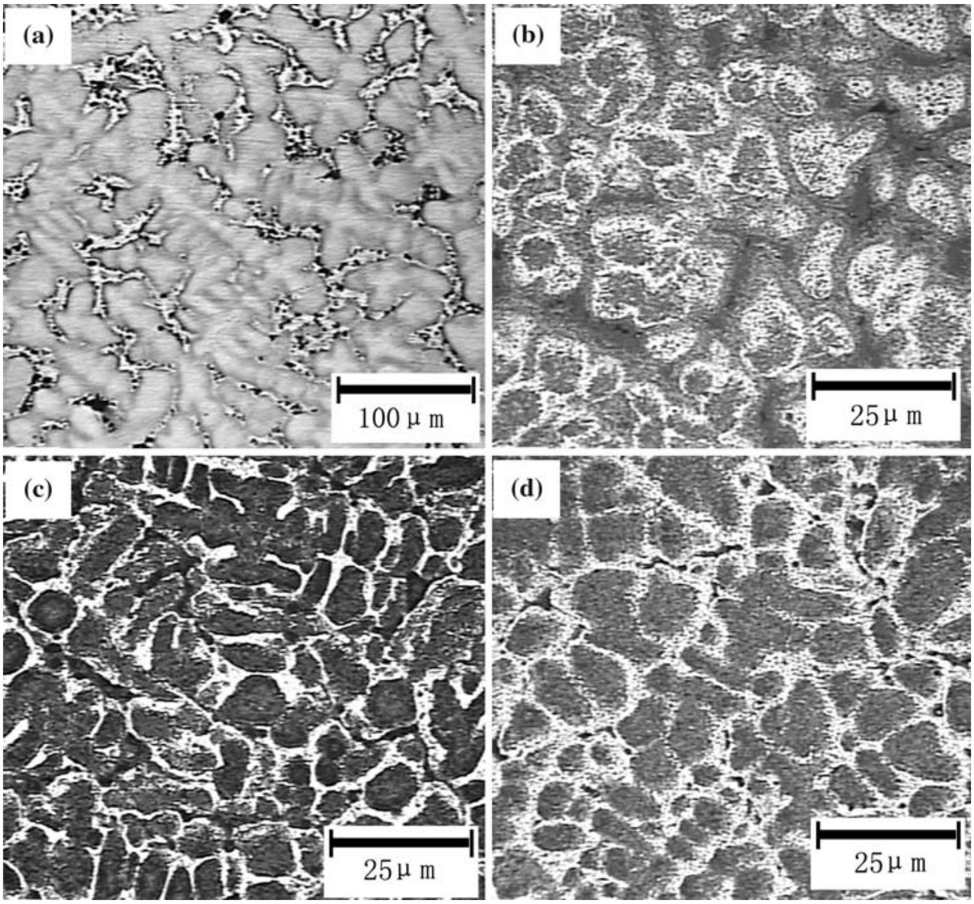

Fig. 1 Original austenite grain of A_0 sample (a), A_1 sample (b), A_2 sample (c), and A_3 sample (d)

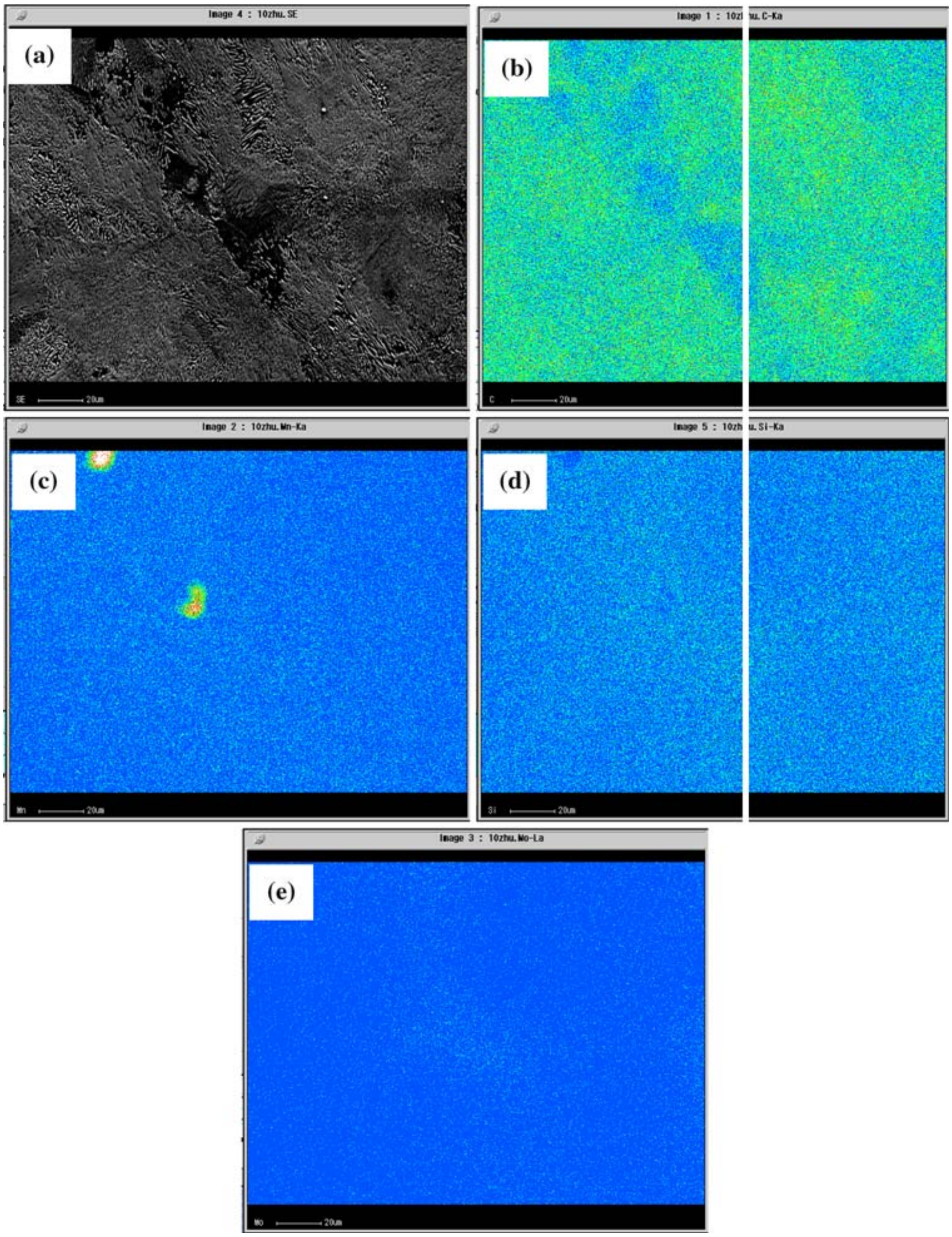

Fig. 2 EPMA analysis of unmodified high carbon alloy cast steel sample. (a) SEM; (b, e) the X-ray images for respective element: C, Mn, Si, and Mo

REEs have low melting points and large atom radius, i.e., $r_{\mathrm{Ce}} = 0.182$ nm. They are all strong ingredient undercooling elements in the solidification of high carbon alloy cast steel. Since the equilibrium constant K_0 is far smaller than 1 (Ref 14), serious segregation occurs during the solidification. A number of elements concentrate in front of the primary austenite through redistribution. This results in high ingredient supercooling, benefits the multiple branching of the austenite crystal, reduces the arm space of dendrites, and refines the primary austenite (Ref 14, 15). In addition, RE can also deoxidize and desulfurize in molten steel, decreasing the contents of sulfur and oxygen by combining them to form rare earth oxide and sulfide. Moreover, vanadium and titanium can combine with carbon and nitrogen in molten steel and form carbon and nitrogen compounds having high melting points (Ref 16, 17). In certain conditions, the rare earth oxide and sulfide and carbon and nitrogen compound can act as the solidification nuclei of molten steel. Moreover, a number of rare earth oxide and sulfide and carbon and nitrogen compounds have been discovered through SEM and EDS, as shown in Fig. 4-6. Because the EDS apparatus only detects elements with an atomic number of 11 or higher, the EDS spectra in Fig. 4-6 cannot reveal the existence of carbon and nitrogen and oxygen.

According to the mismatch theory brought forward by Turnbull (Ref 18), the high melting compound can be a non-spontaneous crystal nucleus of the new crystalline phase due to the mismatch of the two phases' lattice parameter:

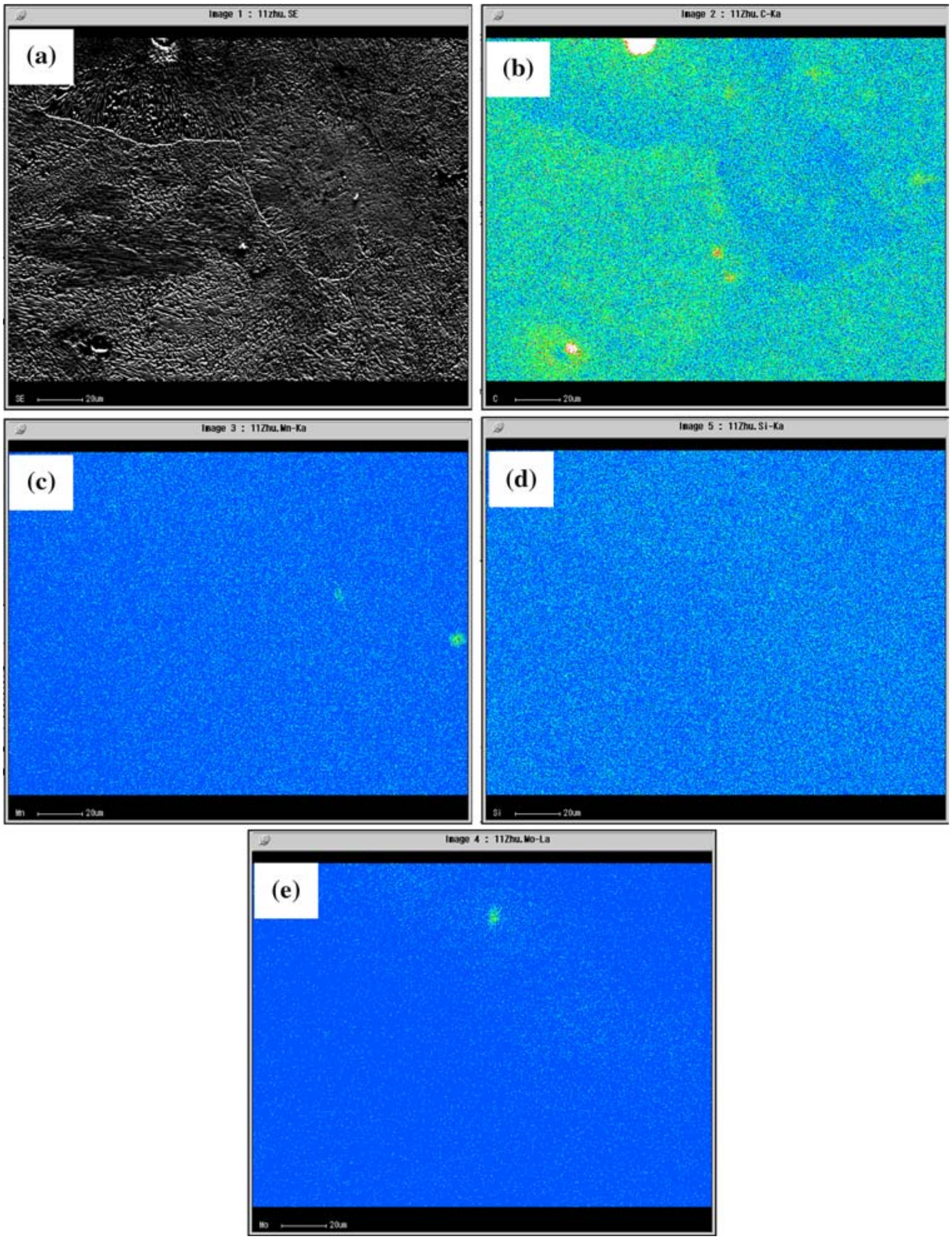

Fig. 3 EPMA analysis of high carbon alloy cast steel sample containing 0.25 wt.% RE and 0.15 wt.% V and 0.15 wt.% Ti. (a) SEM; (b, e) the X-ray images for respective element: C, Mn, Si, and Mo

$$\delta = \frac{a_C - a_N}{a_N} \qquad \text{(Eq 1)}$$

where, δ is the mismatch of lattice parameter, a_C and a_N are low index planes of the substrate and the nucleated solid phase, respectively.

Bramfitt (Ref 19) proposed a theory that the nuclei were most effective when the mismatch was less than 6%, less effective between 6% and 12%, useless above 12%. The rare earth oxide and sulfide and carbon and nitrogen compounds have high melting points and lower mismatch with γ-Fe lattice. For example, the mismatches of RE_2O_3 and, TiN with γ-Fe lattice are 5.0% and 3.9%, respectively. Therefore, RE_2O_3, TiN, etc. can act as the effective heterogeneous nuclei of primary austenite and promote the refinement of as-cast structure.

Moreover, vanadium and titanium can increase the degree of supercooling of molten steel (Ref 20). According to the nucleating rate formula of the molten metal (Ref 21):

$$\mu = \frac{NKt}{h} \exp\left[-\frac{\Delta F_A + \Delta F^*}{kT}\right] \qquad \text{(Eq 2)}$$

where u is the nucleus quantity formed per second per unit volume liquid; N is the total number of atoms per unit volume liquid; k is Boltzmann's constant; h is Planck's constant; T is the absolute temperature; ΔF_A is the activation

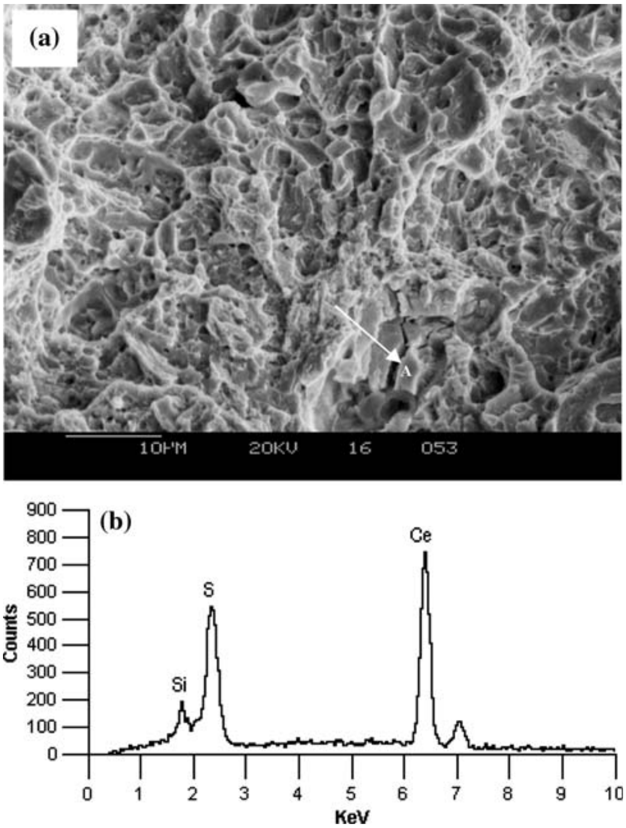

Fig. 4 SEM fractography of A_3 sample (a) and EDS in *A* point (b)

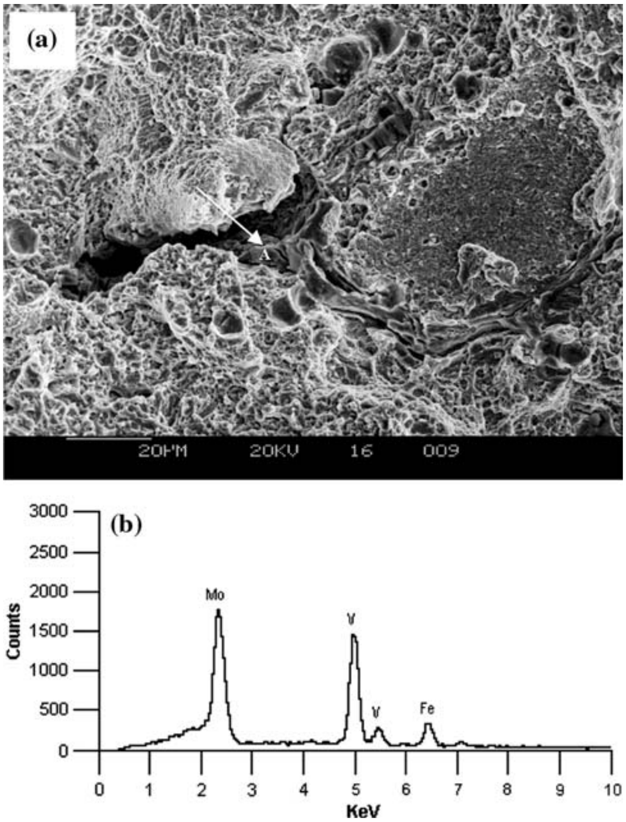

Fig. 5 SEM fractography of A_3 sample (a) and EDS in *A* point (b)

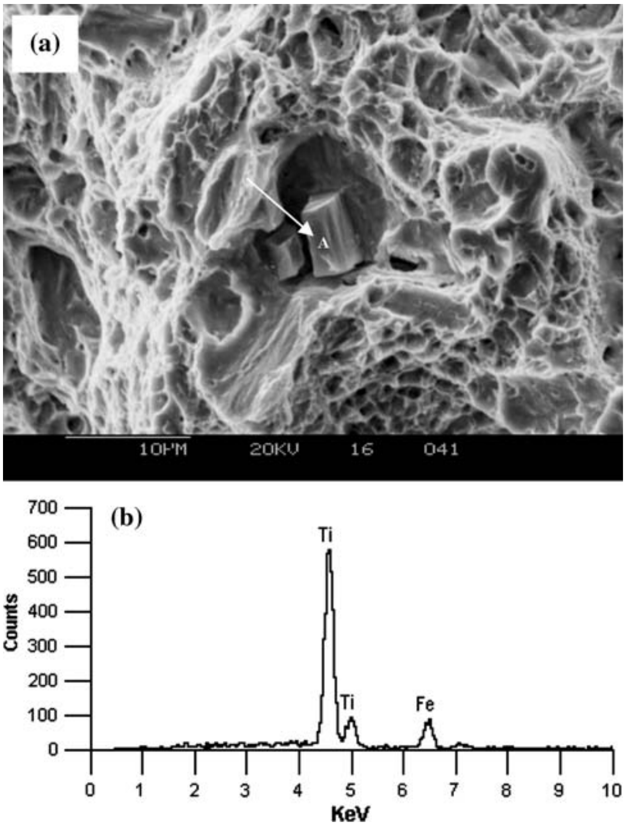

Fig. 6 SEM fractography of A_3 sample (a) and EDS in *A* point (b)

energy of atomic diffusion in molten steel; and ΔF^* is the power of critical nucleation, its value is given as follows (Ref 21)

$$\Delta F^* = \frac{1}{3}\left[\frac{16\pi\sigma_{LS}^3 T^2}{L^2 \Delta T^2}\right] \quad \text{(Eq 3)}$$

where σ_{LS} is the surface energy, N/m; L is the latent heat of crystallization, J/m^3; and ΔT is the degree of supercooling, K.

Formula (2) comprises two portions. As the power of critical nucleation ΔF^* is inversely proportional to ΔT^2, $\exp\left(-\frac{\Delta F^*}{kT}\right)$ increases rapidly with the increase of degree of supercooling, i.e., nucleating rate increases correspondingly. On the other hand, as the degree of supercooling increases, the atomic heat motion becomes weak; this causes the term $\exp\left(-\frac{\Delta F_A}{kT}\right)$ to decrease and reduce the nucleating rate accordingly. Because of the strong mobility of the metal atom under the solidifying condition, the increase of the degree of supercooling will promote the increase of nucleating rate and quicken the solidification in the common casting condition, a fine solidification structure can be obtained.

5. Conclusions

Based on the above results, the following conclusions can be drawn:

(1) The grain of the unmodified high carbon alloy cast steel is coarse and its average size is 80 µm. Adding

0.25 wt.% RE, the grain size of the cast steel decreases obviously and reaches 65 μm. When 0.25 wt.% RE and 0.15 wt.% V and 0.15 wt.% Ti are added into the cast steel, the grain size of the cast steel decreases further, and the average grain size is only 40 μm.

(2) The unmodified high carbon alloy cast steel has obvious elements' segregation. After modification with RE-V-Ti, the segregation of elements shows a lightening tendency.

References

1. H. Aglan, M. Hassan, Z. Liu, M. Bhuyan, and M. Fateh, Fracture Behavior of Bainitic and Pearlitic Rail Steel Webs, *J. Mater. Sci.*, 2004, **39**(13), p 4305–4307
2. K.M. Lee and A.A. Polycarpou, Wear of Conventional Pearlitic and Improved Bainitic Rail Steels, *Wear*, 2005, **259**(1–6), p 391–399
3. F.G. Caballero and H.K.D.H. Bhadeshia, Design of Novel High-strength Bainitic Steels, *Mater. Sci. Forum*, 2003, **426–432**(2), p 1337–1342
4. E.V. Pereloma, I.B. Timokhina, K.F. Russell, and M.K. Miller, Characterization of Clusters and Ultrafine Precipitates in Nb-containing C-Mn-Si Steels, *Scripta Mater.*, 2006, **54**(3), p 471–476
5. K.I. Sugimoto, M. Tsunezawa, T. Hojo, and S. Ikeda, Ductility of 0.1–0.6C-1.5Si-1.5Mn Ultra High-strength TRIP-aided Sheet Steels with Bainitic Ferrite Matrix, *ISIJ Inter.*, 2004, **44**(9), p 1608–1614
6. L.C. Chang, The Rolling/Sliding Wear Performance of High Silicon Carbide-free Bainitic Steels, *Wear*, 2005, **258**(5–6), p 730–743
7. V.T.T. Miihkinen and D.V. Edmonds, Microstructural Examination of Two Experimental High-strength Bainitic Low-alloy Steels Containing Silicon, *Mater. Sci. Technol.*, 1987, **3**(6), p 422–431
8. H.K.D.H. Bhadeshia and D.V. Edmonds, Bainite in Silicon Steels: New Composition-property Approach, Part 1, *Metal. Sci.*, 1983, **17**(9), p 411–419
9. C. Garcia-Mateo and F.G. Caballero, The Role of Retained Austenite on Tensile Properties of Steels with Bainitic Microstructures, *Mater. Trans.*, 2005, **46**(8), p 1839–1846
10. Y. Tomita and T. Okawa, Effect of Microstructure on Mechanical Properties of Isothermally Bainite-transformed 300M Steel, *Mater. Sci. Eng. A*, 1993, **172A** (1–2), p 145–151
11. X.Y. Zhu, T. You, Q. Shi, Y. Zou, and Q. Lin, Effects of Cerium on Microalloying in Low Sulfur Nb-Ti-bearing Steel, *J. Rare Earths*, 2005, **23**(6), p 742–746
12. V.A Lyutyj, E.A. Platonov, G.E. Fedorov, and A.E. Kyz'menko, Chromium Aluminum Steels for Manufacturing Heat-resistant Part for Heat-power Engineering Equipment, *Litejnoe Proizvodstvo*, 2001 (4), p 13–15
13. H.C. Li and W.H. Sun, Industrial Practice of Rare Earth Treatment for Titanium Microalloyed Steel at Jinan Iron and Steel Group Corp, *Iron Steel (Peking)*, 2001, **36**(9), p 19–20
14. G.Y. Liang and J.Y. Su, The Effect of Rare Earth Elements on the Growth of Eutectic Carbides in White Cast Irons Containing Chromium, *Cast Metals*, 1991, **4**(2), p 83–88
15. H. Li, A. McLean, J.W. Rutter, and I.D. Sommerville, Influence of Rare Earth Metals on the Nucleation and Solidification Behavior of Iron and 1045 Steel, *Metall. Trans. B*, 1988, **19B** (3), p 383–395
16. S. Engineer, A Review of the Development and Application of Microalloyed Medium Carbon Steels, *Steel Res.*, 1987, **68**(8), p 369–376
17. R.L. Bodnar, Applications of Titanium Nitride Technology to Steel Products, *Iron Steelmak.*, 1994, **21**(1), p 19–24
18. D. Turnbull and B. Vonnegut, Nucleation Catalysis, *Ind. Eng. Chem.*, 1952, **44**(6), p 1292–1298
19. B.L. Bramfitt, Planar Lattice Disregistry Theory and Its Application on Heterogistry Nuclei of Metal, *Metall. Trans.*, 1970, **1**(7), p 1987–1995
20. S.L. Huang, Experimental Study of Super High Manganese Wear Resistant Cast Steel Modified by RE, Vanadium and Titanium, *Mine Mach.*, 2001, (2), 51–53
21. Q.C. Li, *Theory Base of Casting Formation*, Machinery Industry Press, Beijing, 1982, p 86–93